

Accuracy Investigation of CFC Method for Sensorless Vector Control of Salient Pole Synchronous Motors

Essam Eddin M. Rashad, SMIEEE

*Department of Electrical power and Machines Engineering,
Faculty of Engineering, Tanta University,
Tanta, Egypt*

Email: emrashad@ieeee.org

Abstract. This paper discusses the problems associated with the application of carrier frequency component (CFC) method for sensorless control of salient pole synchronous motors. The method has been successfully applied for low speed range for interior permanent magnet (IPM) motor drive systems. Since the method is a saliency-based technique, it can be applied to both conventional synchronous motor and to the synchronous reluctance (SyncRel) motor drive systems. Implementation of the method for higher speed range shows increase in rotor position estimation error, especially for loaded conditions. This error was mainly attributed to the variation of CFC voltage with rotor position and speed. However this reason does not allow for both the load effect and the employed control method. Therefore, an extensive investigation of CFC method accuracy has been studied and presented in this paper. Accurate analysis of both magnitude and phase of CFC voltage variation is given. Then accuracy of the CFC method is evaluated for different loads and vector control techniques. The results can be implemented to improve the validity and accuracy of CFC sensorless control method

Key words

Sensorless control, vector control, carrier frequency, IPM motor, Synchronous Reluctance Motor.

1. Introduction

Recently, an increasing interest has been given to the sensorless vector control of different types of electric drive systems. For high performance applications, rotor position has to be known in order to perform the field orientation task. The mechanical position sensor represents a considerable part of the drive system cost and volume while it reduces system reliability. Moreover, presence of sensor affects the system dynamic performance. Accordingly, many papers have been published to describe methods for eliminating the mechanical position sensor for all types of electrical motors.

Permanent magnet synchronous motor (PMSM) drives are today gradually replacing classic dc drives in industry applications [1]. Different solutions have been suggested

for sensorless control of PMSM. Three different categories can be distinguished [2]:

1. **Back-emf estimation based techniques**, which use the measured fundamental stator terminal quantities along with the motor model. The methods are simple and suitable for medium and high speeds. Since the method is model-based, variation of parameters have to be considered [2-3]. However, for low speeds, back emf is small and the model uncertainty becomes significant so that the estimation becomes too noisy. This results in unstable operation [4].
2. **State observers and extended Kalman filter (EKF) techniques**, which have found a wide application in sensorless control of PMSM [5-6]. However, these techniques fail at standstill and low speed because the model becomes not observable in these conditions.
3. **Techniques based on the machine's physical properties:** These techniques are based on the stator inductances variations due to the magnetic circuit configuration. They are the only methods capable of determining the rotor position at standstill and very low speeds. The IPM and SyncRel motors are well suited for these techniques because of the inherent large spatial saliency provided by these types of motors. [7-8]

The implementation of the third category is primarily based on injecting a high frequency voltage signal with small amplitude [9-12]. The resulted high frequency current is amplitude modulated according to the spatial saliency.

Due to their advantageous construction, low cost and high reliability, SyncRel motors are replacing other types of motors in many applications. Therefore much research effort has been done for sensorless control of SyncRel motors drive systems. The adopted techniques use position estimator [13-14], high frequency signal injection [15] and combining high-frequency current injection method in the low-speed region and the flux estimation method based on the stator voltages in the high-speed region. [16]

The main drawback of signal injecting is the need for a separate high frequency source. Moreover, signal frequency has to properly chosen [17]. If it is decreased, it may cause torque ripples and acoustic noise. If the frequency approaches the inverter switching frequency, it becomes difficult to filter it out. On the other hand, for a relatively high frequency, the rotor position dependent part of the inductance tends to diminish due to the increase in leakage inductance, which causes a deterioration of estimated rotor position accuracy.

In [18], it is proposed to use the voltage component of carrier frequency inherently existing in sinusoidal pulse width modulated (SPWM) inverter output voltage. This component is called carrier frequency component (CFC) voltage. The resulted CFC current is amplitude modulated such that it can be used to get rotor position information, without the need for a separate high frequency source. Figure 1 shows a block diagram of CFC method. The technique has been successfully applied in IPM motor drive for low speed range. In this case the CFC voltage can be assumed independent of rotor position so that the method has been greatly simplified. Some researchers suggested modified implementation of the method over the whole speed range keeping the assumption of constant CFC voltage [17 & 19].

However, it was noted that position estimation error increases not only with speed but also with load. The error increases significantly for speeds over 0.8 pu specially for loads near rated torque. It was mainly attributed to CFC voltage variation. Accordingly, this variation has been investigated for different speeds and different values of angle between reference triangle waves employed to generate SPWM scheme [20]. The analysis assumes that reference voltage is proportional to the reference speed. This assumption may be acceptable for scalar control (constant V/f) while it is not suitable for vector controlled motor drive. However the given analysis is helpful in determining CFC voltage variation in terms of reference voltage, whatever reference speed is.

This paper presents an extensive investigation of CFC method under different vector control techniques. The main object is to explore method accuracy. More accurate analysis for CFC voltage variation is given. The analysis considers both magnitude and phase values. Effect of both command speed and load torque on position determination error is discussed. Effect of the adopted vector control strategy has been examined and assessed. The results can be implemented to improve the validity and accuracy of CFC sensorless control method

2. Brief Review of CFC Method for Position Estimation

The principle of CFC method will be briefly reviewed in this section [17-20]. Detailed analysis is given in [21]

Under proper assumptions, the motor voltage equation is reduced to the following form when the applied voltage is that of CFC of the PWM inverter output voltage:

$$\mathbf{V}_c = \mathbf{L}(\theta) p \mathbf{I}_c \quad (1)$$

where the subscript ‘‘c’’ stands for ‘‘carrier frequency’’ and $\mathbf{L}(\theta)$ is motor inductance matrix. θ is the rotor position angle

If (1) is transformed into the stationary reference frame α - β , $\cos(\theta)$ and $\sin(\theta)$ can be obtained by demodulating CFC currents.

Digital implementation can be greatly simplified so that the rotor position can be calculated using the following relations:

$$\cos(2\theta) = -\frac{L}{M} + L \int e_\beta dt \quad (2)$$

$$\sin(2\theta) = \frac{L}{M} - L \int (e_\beta + e_\alpha) dt \quad (3)$$

where e_α and e_β are the transformed carrier frequency voltage components.

i_α and i_β are the transformed carrier frequency current components.

$$L = (L_d + L_q)/2 \text{ and } M = (L_d - L_q)/2$$

L_d and L_q are the stator d- and q- axes inductances, respectively

θ is the rotor position angle

Moreover, using (2 & 3) can be simplified if the following assumptions are accepted:

- e_α , e_β and $(e_\alpha + e_\beta)$ are constants.
- e_α and e_β are 90° out of phase.

Investigation of all adopted assumptions shows that they are acceptable only for low speed operation.

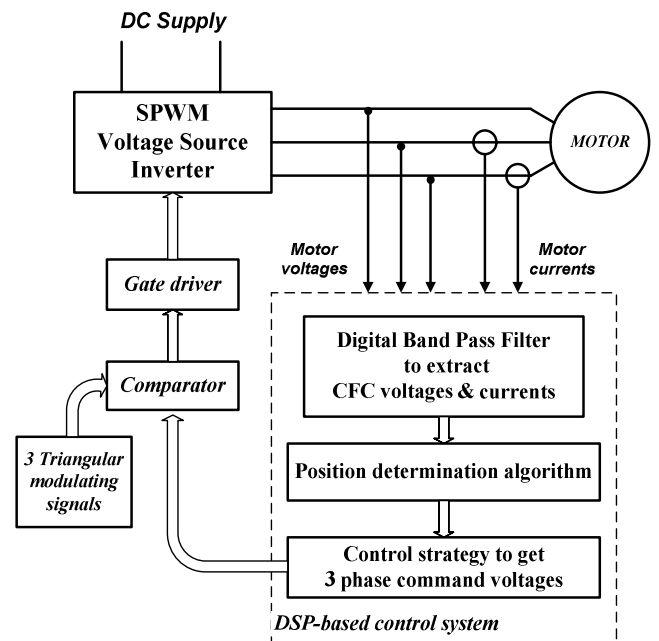


Fig. 1 Simplified block diagram of the CFC method for sensorless control of salient pole motors.

3. Characteristics of CFC voltage

The command voltage is determined according to the control strategy. For balanced three phase command voltage, the fundamental component of phase 'a' voltage is given by:

$$v_a = V_m \sin(\omega t) \quad (4)$$

where V_m and ω are the supply maximum voltage and frequency respectively.

The variation of CFC voltage with rotor position have been derived before [20] assuming that the command voltage in constant within one carrier cycle. This assumption may result in inaccurate results when the ratio between supply and carrier frequencies becomes relatively. This is the condition at high speeds. The same problem may result when the employed carrier frequency is relatively low

For more accurate determination of CFC voltage variation, the command voltage has been assumed varying linearly within one carrier cycle. Assume that:

- E is the inverter dc link voltage.
- ω_c is the carrier angular frequency ($=2\pi f_c$).
- The three triangular waves employed to generate SPWM inverter switching signals are equi-shifted.
- Magnitude of triangle waves is scaled so that it corresponds to E . This means that V_m does not exceed E to avoid over modulation.
- m_a is pu command voltage and m_f is the ratio between carrier and supply frequencies.

Fig. 2 can be used to derive the magnitude and phase angle of CFC voltages.

The CFC voltages are of balanced. Normalized (divided by $-2E/\pi$) CFC voltages are given by:

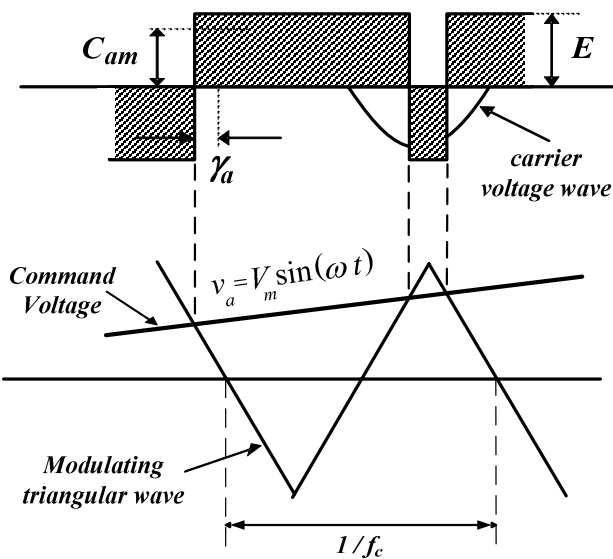


Fig. 2 Time relation between triangular modulating wave, command instantaneous voltage, carrier voltage wave and inverter output for phase 'a'.

$$v'_{ca} = C_{am} \sin(\omega_c t + \gamma_a) \quad (6a)$$

$$v'_{cb} = C_{bm} \sin(\omega_c t - 2\pi/3 + \gamma_b) \quad (6b)$$

$$v'_{ca} = C_{cm} \sin(\omega_c t + 2\pi/3 + \gamma_c) \quad (6c)$$

where C_{am} , C_{bm} & C_{cm} are the normalized peak values, and γ_a , γ_b & γ_c are phase shift (drift) between a carrier voltage wave and the corresponding triangle wave.

C_{am} and γ_a are given by the following relations:

$$C_{am} = \cos[(x_1 + x_2)/2] \quad (7)$$

$$\gamma_a = \tan^{-1} \left(\frac{\sin x_2 - \sin x_1}{\cos x_2 + \cos x_1} \right) \quad (8)$$

where: $x_1 = m_a V_m \sin(\omega_c t)$ $x_2 = m_a V_m \sin(\omega_c t + \pi/m_f)$

m_a is pu command voltage and m_f is the ratio between carrier and supply frequencies.

Similarly C_{bm} , C_{cm} , γ_b and γ_c can be obtained.

For low values of command voltage magnitude V_m , C_{am} , C_{bm} and C_{cm} will be constant while γ_a , γ_b and γ_c tend to zero. If a command voltage within one carrier period is assumed constant, γ_a , γ_b & γ_c are all zero for all values of V_m .

Figure 3 shows the variations of C_{am} , C_{bm} & C_{cm} along with the variation of γ_a , γ_b & γ_c with rotor position a command voltage of 0.6 pu. Fig. 4 shows the variation of C_{am} & γ_a for different values of command voltages. It is that variation of CFC voltage can not be neglected for relatively high values of command voltages. Moreover, drift angle increase results which may affect the method accuracy.

4. Voltage Command Requirement Analysis

The effect of loading depends on the adopted control strategy, which determines the value of required command voltage V^* to satisfy the desired speed for a certain load torque. Each value of the developed torque T_e has corresponding pairs of V^* and load angle δ .

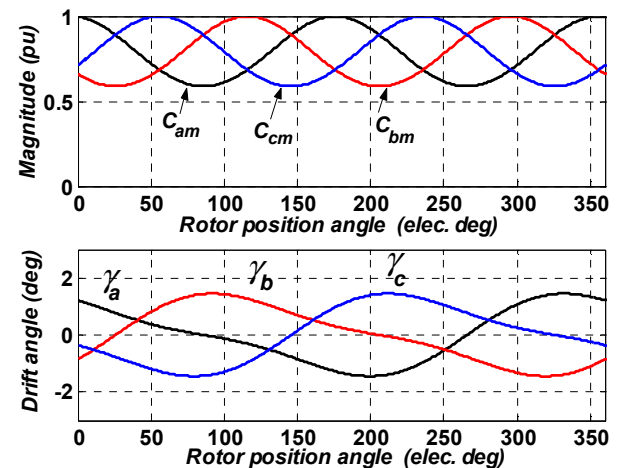


Fig. 3 variation of CFC voltages magnitude and drift angles for a command voltage of 0.6 pu.

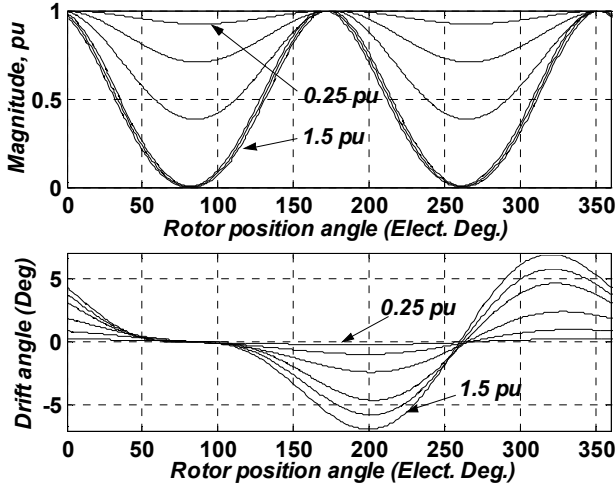


Fig. 4 variation of one of CFC voltage magnitude and its drift angle for command voltages from 0.25 to 1.5 pu with 0.25 pu step.

A. Steady-state equations of IPM and SyncRel motors

For IPM motors, the steady state model in rotor reference frame is given by:

$$v_d = R_s i_d - X_q i_q \quad (9)$$

$$v_q = R_s i_q + X_d i_d + \omega \lambda_m \quad (10)$$

where v_d , v_q , i_d and i_q are d and q axes transformed voltages and currents. They are all dc quantities. X_d and X_q are d and q axes reactances at supply frequency ω

The developed torque T_e is given by:

$$T_e = (3P/4) [(L_d - L_q) i_d i_q + i_q \lambda_m] \quad (11)$$

where L_d and L_q are d and q axes inductances. λ_m is flux due to the permanent magnet.

Phase voltage and current can be obtained as follows:

$$V_{ph} = \sqrt{(v_d^2 - v_q^2)/2} \quad \text{and} \quad I_{ph} = \sqrt{(i_d^2 - i_q^2)/2} \quad (12)$$

For IPM motors, $L_d < L_q$, while for SyncRel $L_d > L_q$ in addition to setting λ_m to zero. Therefore the same mathematical model can be used for both motors with the proper parameters.

B. Control strategies

The present analysis deals with three common control strategies; namely:

1. $I_d=0$ control

This strategy is employed for IPM motor to achieve linear control. The q-axis current is determined by the required torque T_e according to (11). Hence v_d and v_q can be obtained from (9) and (10) respectively. Finally V^* can be obtained from (12)

2. Maximum Torque per ampere (MTPA) control

This strategy is implemented to minimize copper loss. The condition of MTPA can be achieved by controlling i_d according to the following relation [22]:

$$i_d = \frac{\lambda_m}{2(L_d - L_q)} - \sqrt{\frac{\lambda_m^2}{4(L_d - L_q)} + i_q^2} \quad (13)$$

3. Flux weakening control

If the desired speed requires exceeding the inverter voltage capability, some flux weakening method has to be used. Keeping the motor command voltage constant at its maximum value, the following i_d - i_q relation has to be achieved by a proper control [22]:

$$i_d = -\frac{\lambda_m}{L_d} + \frac{1}{L_d} \sqrt{\frac{V_m^2}{\omega^2} - (L_q i_q)^2} \quad (14)$$

where V_m is the maximum available supply voltage

C. Voltage Command Requirements

Applying the previous control requirements, the motor variables (such as currents, voltages, torque, power ...etc) can be obtained. In the present analysis, the most important quantities are the command voltage V^* and the load angle δ . Their values are determined according to the command speed, load torque for a specific control strategy. Figure 5 shows the variation of both V^* and δ with the developed torque for different values of command speed under $I_d=0$ vector control. Fig. 6 shows the same relations when applying MTPA control. Fig. 7 shows the variation of δ under the influence of flux weakening control, where V^* is kept at 1 pu. Parameters of the adopted IPM motor are given in the Appendix Section

5. Position Error Investigation

The IPM motor dynamic equations have been implemented under the application of CFC voltages according to the previous analysis. The input to the program is V^* and δ , which correspond to a certain operating point (determined by the load torque, command speed and the control method). The rotor position has been estimated using the CFC method and compared with the actual position to get the estimation error.

Define:

θ is the actual rotor position angle.

θ_{est} is the estimated rotor position angle.

Then the rotor position error can be defined as follows:

$$er = \text{abs}(\theta - \theta_{est}) \quad (13)$$

and

er_{max} is the absolute value of the maximum er over one revolution

er_{av} is the average value of $\text{abs}(er)$ over one revolution

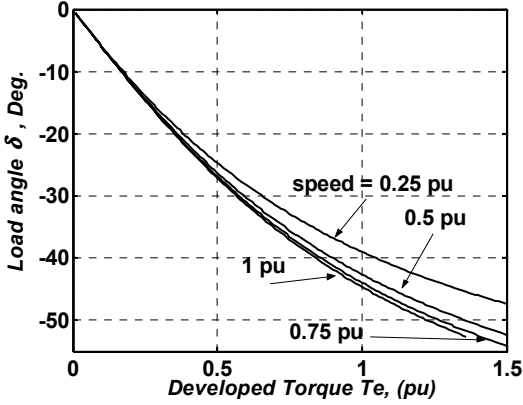
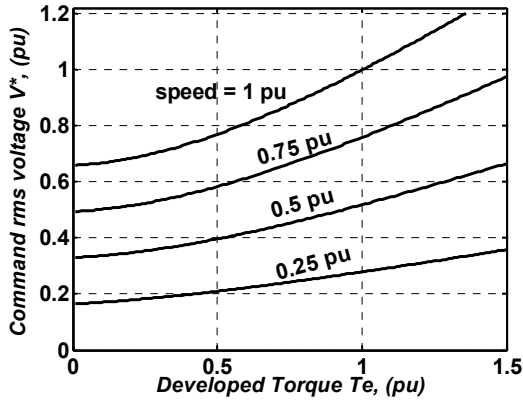


Fig. 5 Variation of command voltage (upper) and load angle δ (lower) with load torque at different pu speeds for $I_d=0$ control strategy.

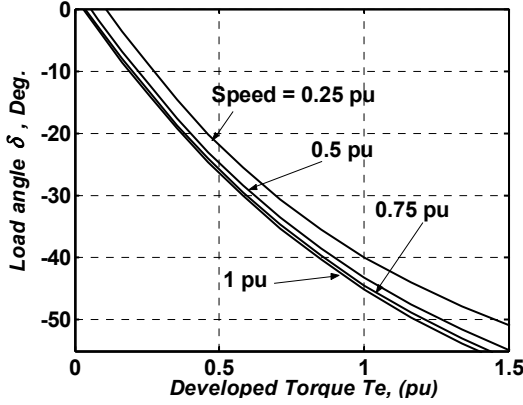
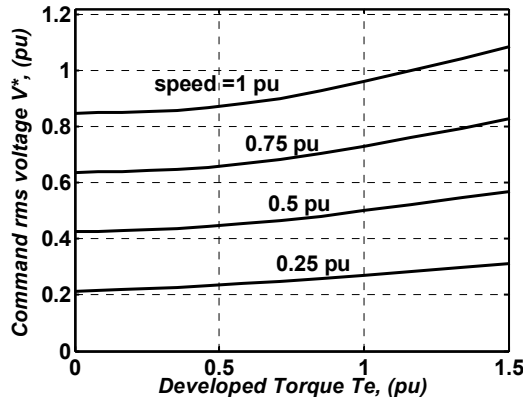


Fig. 6 Variation of command voltage (upper) and load angle δ (lower) with load torque at different pu speeds for MTPA control strategy.

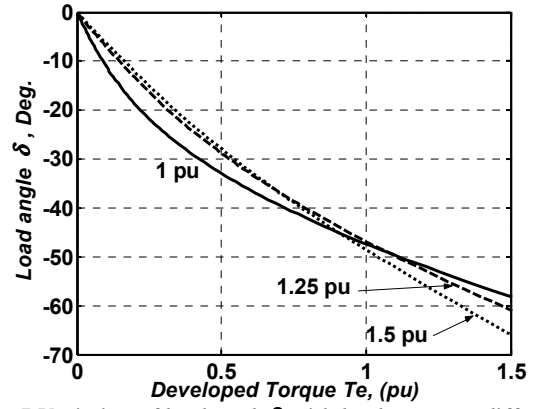


Fig. 7 Variation of load angle δ with load torque at different pu speeds for flux weakening control strategy.

Table I summarizes some of the attained results. Figure 8 shows samples of the estimated rotor position angle variation for different cases.

Table I Error of rotor position estimation for different cases

Control strategy	Speed (pu)	T_e (pu)	V^* (pu)	δ (deg)	er_{max} (deg)	er_{av} (deg)
$I_d=0$	0.25	0.25	0.183	-13.9	12.3	7.7
		0.5	0.21	-24.7	12.75	7.77
		1	0.279	-39	14.02	7.8
		1.25	0.318	-43.7	14.65	7.75
	1	0.25	0.695	-14.7	33.34	14.12
		0.5	0.77	-27.1	42.05	21.97
		1	1.00	-44.7	39.26	25.69
		1.25	1.138	-50.5	33.06	23.85
MTPA	0.25	0.25	0.223	-8.75	12.37	7.8
		0.5	0.234	-21.8	13.06	7.85
		1	0.27	-39.8	13.89	7.78
		1.25	0.291	-45.9	14.18	7.71
	1	0.25	0.854	-13.5	69.74	34.69
		0.5	0.872	-26.3	53.59	30.3
		1	0.961	-45	38.72	24.62
		1.25	1.021	-51.6	33.67	22.44
Flux weakening	1	0.25	1	-21.7	68.71	39.27
		0.5	1	-32.9	52.34	32.77
		1	1	-47.4	37.1	24.25
		1.25	1	-53	32.35	21.34
	1.25	0.25	1	-16.3	80.24	42.98
		0.5	1	-28.8	60.23	35.85
		1	1	-46.2	39.56	25.9
		1.25	1	-54.2	33.07	21.42

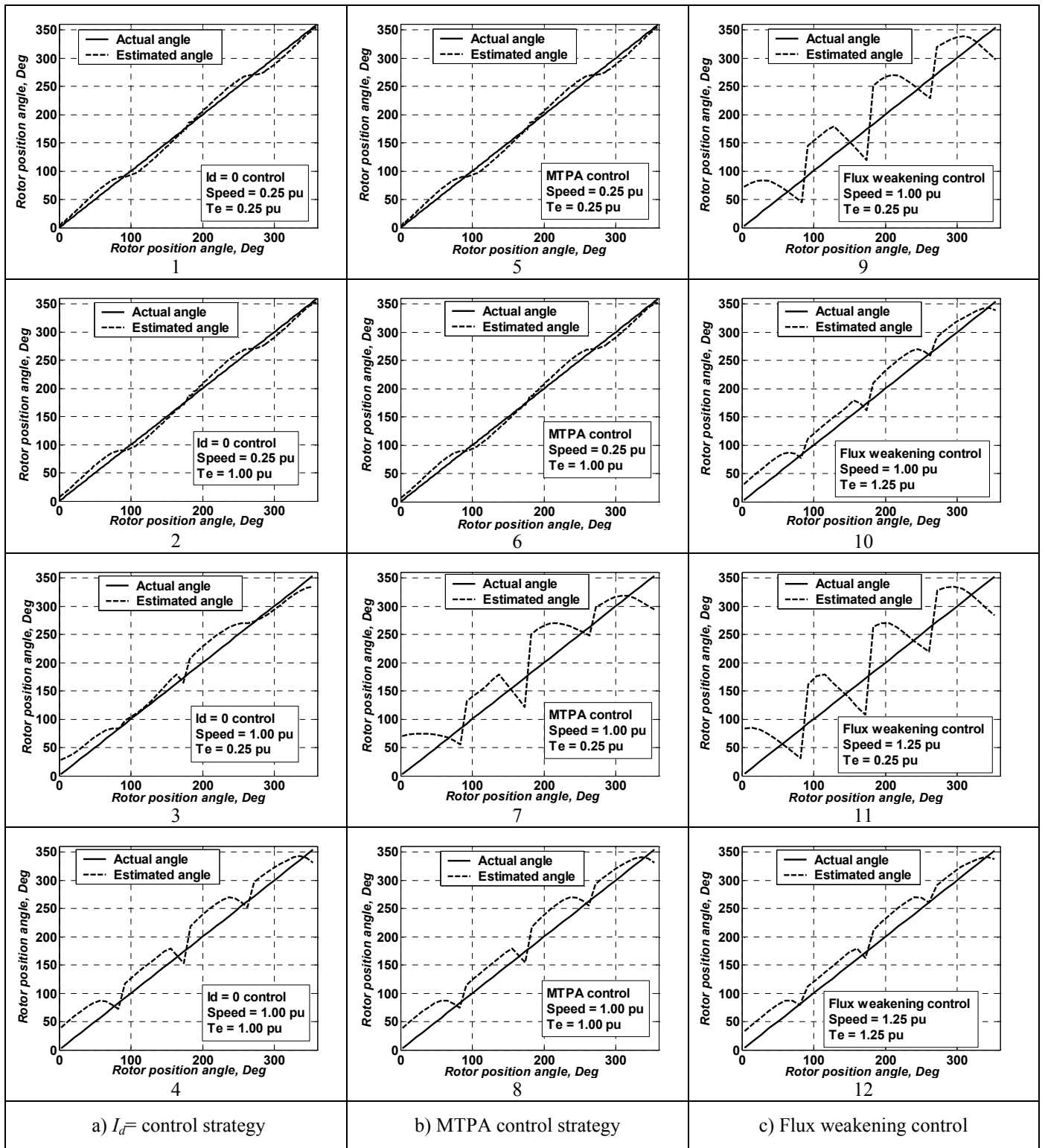


Fig. 8 Variation of estimation error along one revolution for sample cases.

From Table I, the combined effect of speed, command voltage (V^*) and load angle (δ) is noted. The following notes may be obtained:

1. As known, for low speed operation, error is relatively low for all loads (V^* and δ) and proper control strategy.
2. For the same value of $|\delta|$ and speed, error increases with increase in V^* . This note can be clarified when comparing the following three cases of approximately same δ :

- ⇒ I_d control, speed = 0.25 pu and $T_e = 0.25$ pu.
- ⇒ I_d control, speed = 1.00 pu and $T_e = 0.25$ pu.
- ⇒ MTPA control, speed = 1.00 pu and $T_e = 0.25$ pu.

Rows of the three cases are shown shaded in Table I. It is noted that error increases (7.7, 14.12, 34.69 respectively) with increase in V^* (0.183, 0.695, 0.854 respectively)

3. Estimation error increases with loading for I_d control when speed = 1 pu, while it decreases with loading at the

same speed for MTPA control. In both cases, range of δ is the same. This may be attributed to that the corresponding V^* range is relatively higher for MTPA (0.854-1.021 pu) than that for I_d control (0.695–1.138 pu).

4. For the same V^* and speed, error decreases with the increase in $|\delta|$. That is obvious from the given data for the flux weakening operation, where error decreases with loading (increasing $|\delta|$)

Effect of load angle δ on the estimation accuracy can be justified as follows:

- If CFC voltage is constant, the variation of CFC current modulation is determined only by the magnetic circuit saliency.
- If CFC voltage is also modulated, the load angles will affect the relative space location of pole with respect to the CFC voltage peak modulation. There are two extreme conditions:
 - The first condition is when poles (d-axes i. e high reluctance and low reactance) face the peak modulation. In this case CFC current modulation is high, which means higher difference between maximum and minimum modulated CFC currents. Hence the estimation resolution is increased.
 - The second extreme condition is in reverse sense to the first, resulting in low estimation resolution and more error possibility

For more clarification, Figs. 9-10 show the effect of V^* , δ and speed on estimation average error (er_{av}). These figures clarify that the estimation error increases with:

- increase in speed
- increase in command voltage
- decrease in load angle magnitude

Again, it should be emphasized that a certain operating point - on any curve in Figs. 9-10 - is determined by the load and the control strategy. Therefore, some ranges in these curves are not practical in terms of the control strategies discussed before. However, results shown in Figs 9-10 may be useful when applying other control schemes.

5. Conclusion

An extensive accuracy investigation of CFC method for sensorless control of salient pole synchronous motors has been presented. Firstly, variation of CFC voltage has been analyzed more accurately. Then command voltage requirement has been analyzed for different vector control techniques. Hence, the CFC method has been applied to obtain the rotor position angle. The results have been compared with the actual angle to get the error. The following conclusions can be extracted from the given analysis and investigation:

- As known before, the CFC voltage varies with rotor position. Moreover, it varies with command voltage, not with command speed as thought before.
- For higher command voltage, CFC voltage has a drift angle from the zero value assumed in the previous work.

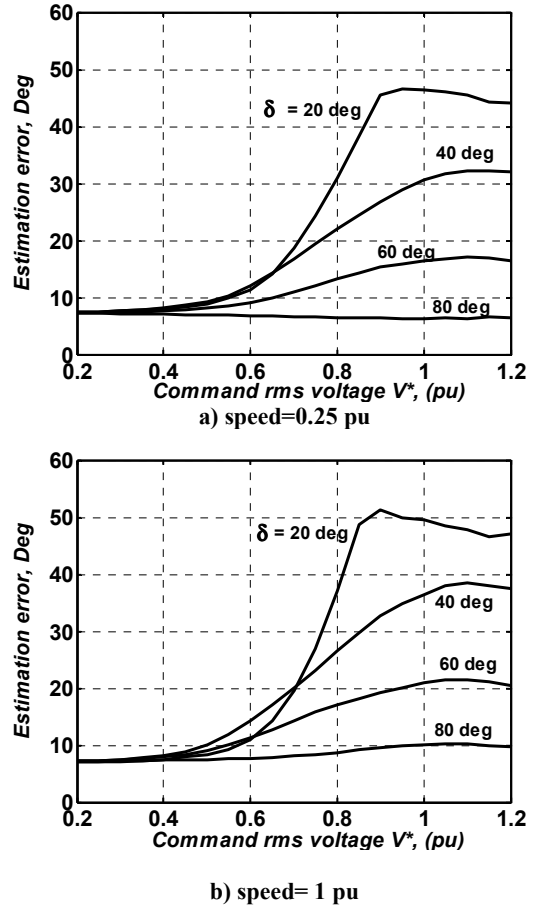


Fig. 9 Effect of command voltage V^* on estimation error for different values of load angle δ

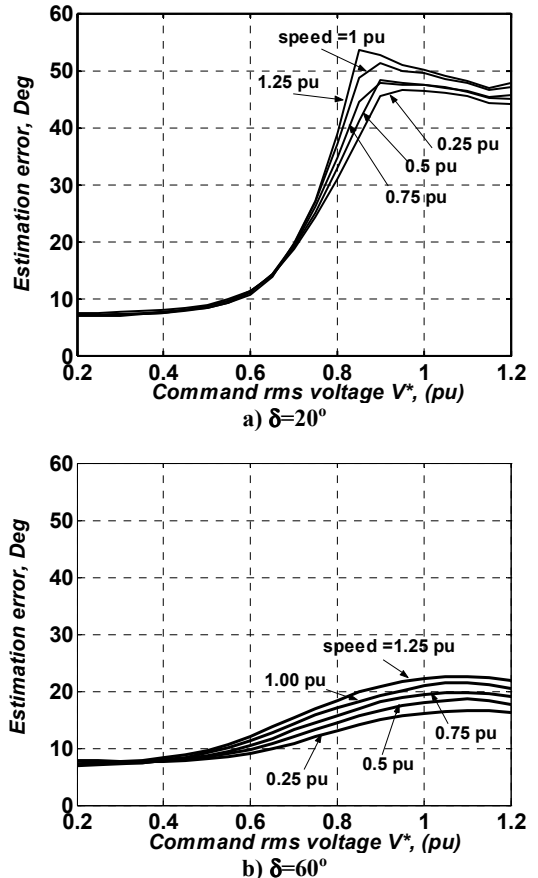


Fig. 10 Effect of command voltage V^* on estimation error for different values of speed

- When applying CFC method for sensorless control, CFC voltage variation can not be neglected for high values of command voltages. Moreover, the resulted phase shift (drift) may affect the method accuracy.
- Rotor position estimation error is not only affected by command speed, but also with command voltage and load angle. These values are determined by both load and the employed control strategy.
- The estimation error increases with increase in speed, increase in command voltage and decrease in load angle magnitude.

In spite of the previous restrictions, CFC method can be considered one of the simplest techniques for sensorless vector control of salient pole synchronous motors. It is important to integrate the effects discussed in this paper into the rotor position estimation algorithm. This may be done by proposing suitable techniques to compensate for the source of errors.

Appendix

Parameters of the adopted IPM motors:

$$R_s=1.93 \Omega; L_d = 0.04244 \text{ H}; L_q=0.07957 \text{ H};$$

$$\lambda_m =0.314 \text{ Wb}; \text{Number of poles} = 4.$$

Rated speed= 1800r/min. Rated torque=3.96 Nm.
Rated phase current =3 A

References

- [1] A. Consoli, G. Scarcella and A. Testa, "Industry Application of Zero-Speed Sensorless Control Techniques for PM synchronous Motors"; *IEEE Trans. on Industry Applications*, Vol. 37, No. 2, Sept. 2001, pp. 513-521
- [2] B. N. Mobarakeh, F. M. Tabar and F. M. Sargos, "Mechanical Sensorless Control of PMSM With Online Estimation of Stator Resistance" *IEEE trans. on Industry Applications*, Vol. 40, No. 2, march/april 2004, pp. 457-471
- [3] K.Y. Cho, S.B. Yang and C.H. Hong, "Sensorless control of a PM synchronous motor for direct drive washer without rotor position sensors", *IEE Proc.-Electr. Power Appl.*, Vol. 151, No. 1, January 2004, pp. 61-69
- [4] S. Ostlund and M. Brokemper, "Sensorless Rotor Position Detection from Zero to Rated Speed for an Integrated PM synchronous Motor Drive", *IEEE Trans. on Industry Applications*, Vol. 32, No. 5, Sept/Oct. 1996, pp. 1158-1165
- [5] S. Bolognani, R. Oboe, and M. Zigliotto, "Sensorless full-digital PMSM drive with EKF estimation of speed and rotor position," *IEEE Trans. on Industrial Electronics*, Vol. 46, No. 1, Feb. 1999, pp. 184-191.
- [6] Yoon-Ho Kim and Yoon-Sang Kook, "High Performance IPMSM Drives without Rotational Position Sensors Using Reduced-Order EKF", *IEEE Transactions on Energy Conversion*, Vol. 14, No. 4, December 1999, pp. 868-873
- [7] S. Ogasawara and H. Akagi, "An Approach to Real-Time Position Estimation at Zero and Low Speed for a PM Motor Based on Saliency", *IEEE Trans. on Industry Applications*, Vol.34, No. 1, Jan./Feb. 1998, pp. 163-168
- [8] S. Shinnaka, "New "Mirror-Phase Vector Control" for Sensorless Drive of Permanent-Magnet Synchronous Motor With Pole Saliency", *IEEE Trans. on Industry Applications*, Vol. 40, No. 2, March/April 2004, pp 599-606
- [9] P. L. Jansen and R. D. Lorenz, "Transducerless Position and Velocity Estimation in Induction and Salient AC Machines", *IEEE Trans. on Industry Applications*, Vol. 31, No. 2, March/April 1995, pp. 240-247
- [10] Ji-Hoon Jang, Seung-Ki Sul, Jung-Ik Ha, K. Ide and M. Sawamura, "Sensorless Drive of Surface-Mounted Permanent-Magnet Motor by High-Frequency Signal Injection Based on Magnetic Saliency", *IEEE Trans. on Industry Applications*, Vol. 39, No. 4, July/Aug. 2003, pp. 1031-1039
- [11] Ji-Hoon Jang, Jung-Ik Ha, M. Ohto, K. Ide and Seung-Ki Sul "Analysis of Permanent-Magnet Machine for Sensorless Control Based on High-Frequency Signal Injection", *IEEE Trans. on Industry Applications*, Vol. 40, No. 6, Nov./Dec. 2004, pp. 1595-1604
- [12] Yu-Seok Jeong, R. D. Lorenz, T. M. Jahns and Seung-Ki Sul, "Initial Rotor Position Estimation of an Interior Permanent-Magnet Synchronous Machine Using Carrier-Frequency Injection Methods", *IEEE Trans. on Industry Applications*, Vol. 41, No. 1, Jan./Feb. 2005, pp. 38-45
- [13] P. Ciufò and D. Platt, "Sensorless rotor position and speed estimation for a synchronous reluctance motor" *IEE Proc. Electr. Power Appl.*, Vol. 150, No. 2, Mar. 2003. pp.158-164
- [14] Ching-Guo Chen, Tian-Hua Liu, Ming-Tsan Lin and Chih-An Tai, "Position Control of a Sensorless Synchronous Reluctance Motor", *IEEE Trans. on Industrial Electronics*, Vol. 51, No. 1, Feb. 2004, pp. 15-25
- [15] A. Consoli, F. Russo, G. Scarcella and A. Testa, "Low-and Zero-Speed Sensorless Control of Synchronous Reluctance Motors", *IEEE Trans. on Industry Applications*, Vol. 35, No. 5, Sept. 1999, pp. 1050-1057
- [16] Jung-Ik Ha, Seog-Joo Kang and Seung-Ki Sul, "Position-Controlled Synchronous Reluctance Motor Without Rotational Transducer", *IEEE trans. on Industry Applications*, Vol. 35, No. 6, Nov/Dec. 2004, pp. 1393-1398
- [17] Mengesha Mamo, Kozo Ide, Mitsujiro Sawamura Jun Oyama, "Novel Rotor Position Extraction based on Carrier Frequency Component Method (CFCM) using Two Reference-frames for IPM drives" in *Proc. of the 27th Annual Conference of the IEEE Industrial Electronics Society (IECON'01)*, held in Denver, Colorado, USA, 29 Nov-2 Dec, 2001
- [18] M. Mamo, J. Oyama, T. Abe, T. Higuchi and E. Yamada, "Carrier frequency component method for position sensorless control of IPM motor in lower speed range", *Trans. of IEE of Japan(IEEJ) on Industry Applications*, Vol. 120-D, No. 2, 2000, pp. 275-280
- [19] J. Oyama, K. Ogawa, T. Higuchi, E. M. Rashad, M. Mamo and M. Sawamura, "Sensorless vector control of IPM motor over whole Speed range", in *Proc. of the International Conference on Power Electronics and Drives Systems (PEDS)*, held in Bali, Indonesia, Oct. 2001, pp. 448-451
- [20] E. M. Rashad, J. Oyama and M. Mamo, "Analysis of Carrier Frequency Component Voltage of sinusoidal PWM inverter for Sensorless Control of IPM Motors", in *Proc. of the 9th annual IEEE-Technical Exchange Meeting*, 16-17 April 2002, KFUPM, Saudi Arabia.
- [21] M. Mamo. " Sensorless Control of Interior Permanent Magnet (IMP) Motors by Carrier Frequency Component Method (CFCM)", PhD Dissertation, Ngasaki University, Japan, 1999
- [22] S. Morimoto, M. Sanada and Y. Takeda, "Wide-Speed Operation of Interior Permanent Magnet Synchronous Motor with High Performance Current Regulator", *IEEE Trans. on Industry Applications*, Vol. 30, No. 2, July/Aug. 1994, pp 920-926